TITLE: Test Cases for a Clipped Delta Wing with Pitching and Trailing-Edge Control Surface Oscillations

9E. TEST CASES FOR A CLIPPED DELTA WING WITH PITCHING AND TRAILING-EDGE CONTROL SURFACE OSCILLATIONS

Submitted by

Robert M. Bennett
Senior Aerospace Engineer
Aeroelasticity Branch, Materials and Structures
Mail Stop 340
NASA Langley Research Center
Hampton, VA 23681-2199 USA
r.m.bennett@larc.nasa.gov

INTRODUCTION

Steady and unsteady measured pressures for a Clipped Delta Wing (CDW) undergoing pitching oscillations and trailing-edge control surface oscillations have been presented in Ref 1 and 2. From the several hundred compiled data points, 22 static cases, 12 pitching-oscillation cases, and 12 control-surface-oscillation cases have been proposed for Computational Test Cases to illustrate the trends with Mach number, reduced frequency, and angle of attack.

The planform for this wing was derived by simplifying the planform of a proposed design for a supersonic transport which is described (Ref 3) as the Boeing 2707-300. The strake was deleted, the resulting planform was approximated by a trapezoid with an unswept trailing edge, and the twist and camber were removed. In order to facilitate pressure instrumentation, the thickness was increased to 6 percent from the typical 2.5 to 3 percent for the supersonic transport. The airfoil is thus a symmetrical circular arc section with t/c = 0.06. A wing of similar planform but with a thinner airfoil of t/c = 0.03 was used in the flutter investigations of Ref 4 and 5, and the buffet and stall flutter investigation of Ref 6. Flutter results are also reported both for the 3 per cent thick simplified wing and for a more complex SST model in Ref 7.

One of the consequences of the increased thickness of the clipped delta wing is that transonic effects are enhanced for Mach numbers near one. They are significantly stronger than would be the case for the thinner wing. Also, with the combination of high leading edge sweep of 50.5° and the sharp leading edge, a leading edge vortex forms on the wing at relatively low angles of attack, on the order of three degrees. The Appendix of Ref 1 discusses some of the vortex flow effects. In addition, a shock develops over the aft portion of the wing at transonic speeds such that at some angles of attack, there is both a leading edge vortex and a shock wave on the wing. Such cases are a computational challenge. Some previous applications of this data set have been for the evaluation of an aerodynamic panel method (Ref 8) and for evaluation of a Navier-Stokes capability (Ref 9-11). Linear theory and panel method results are also presented in Ref 1, which demonstrated the need for inclusion of transonic effects. Flutter calculations for the related wing with t/c=0.03 are given in Ref 4 and 12.

In this report several Test Cases are selected to illustrate trends for a variety of different conditions with emphasis on transonic flow effects. An overview of the model and tests are given, and the standard formulary for these data is listed. For each type of data, a sample table and a sample plot of the measured pressures are presented. A complete tabulation and plotting of the Test Cases is given in Ref 13. Only the static pressures and the1st harmonic real and imaginary parts of the pressures are available. All of the data for the test are included in a microfiche document in the original report (Ref 1) and are available in electronic file form. The Test Cases are also available as separate electronic files.

LIST OF SYMBOLS AND DEFINITIONS

c	local chord, ft (m)
c_r	wing root chord, ft (m)
C_p	pressure coefficient, $(p - p_\infty) / q_\infty$ steady; $(p - p_{mean}) / q_\infty$ unsteady
f	frequency, Hz
H_o	freestream total pressure, psf (kPa)
k	reduced frequency, $\omega c_r/(2V_\infty)$
M	Mach number
p	pressure, psf (kPa)
p_{mean}	mean local pressure, psf (kPa)
p_∞	freestream static pressure, psf (kPa)
q_∞	dynamic pressure, psf (kPa)
R_N	Reynolds number based on average chord
s	semispan, ft (m)

t/c	airfoil thickness to chord ratio
T_o	total or stagnation temperature, °R (°C)
V_∞	freestream velocity, ft/sec (m/sec)
x/c	streamwise fraction of local chord
y	spanwise coordinate normal to freestream
α_o	mean angle of attack, degrees
θ	amplitude of pitch oscillations, degrees or radians
δ	amplitude of control surface oscillations, degrees or radians
δ_o	mean control surface deflection, degrees or radians
η	fraction of span, y/s
γ	ratio of specific heats for test gas
ω	frequency, radians/second

MODEL AND TESTS

The clipped delta wing model was tested in the NASA Langley Transonic Dynamics Tunnel (TDT). The tunnel has a slotted test section 16-feet (4.064 m) square with cropped corners. At the time of these tests, it could be operated with air or a heavy gas, R-12, as a test medium at pressures from very low to near atmospheric values. Currently the TDT can be operated with air or R-134a as a test medium. An early description of this facility is given in Ref 14 and the early data system is described in Ref 15. More recent descriptions of the facility are given in Ref 16 and 17, and of the recent data system given in Ref 18 and 19. Based on cone transition results (Ref 20-21), the turbulence level for this tunnel is in the average large transonic tunnel category. Some low speed turbulence measurements in air have also been presented in Ref 22.

The model is shown installed in the TDT in Fig 1, the basic structure is illustrated in Fig 2, and the overall planform and instrumentation layout is given in Fig 3. It was mounted on a splitter plate offset from the wall. The model had an end plate fixed to its root that moved with the model. To prevent leakage between the end plate and the splitter plate, the region where the splitter plate overlapped the end plate was sealed. The leading edge control surface shown in Figs 1 and 2 was fixed and the side edges smoothly faired into the wing. The hinge line at 15 per cent chord was sealed but not smoothed. The trailing-edge control surface (Figs 1-3) had a hinge line at 80 per cent chord that was sealed but not smoothed. The side edges were not sealed. The model was oscillated in pitch as a mass-spring system with a large spring mechanism located behind the tunnel wall that was driven hydraulically. It could be set at various mean angles, and the amplitude and frequency of oscillation varied. The trailing edge control surface was oscillated with a miniature hydraulic actuator located within the wing at the control surface and attached directly to the shaft along the control hinge line.

The wing was constructed with stainless steel ribs and spars and Kevlar-epoxy skins. Although no stiffness measurements were made, it was considered very stiff. Based on accelerometer measurements, the wind-off node lines showed only modest variation with frequencies in the range of interest (Fig 4). The control surface was constructed with ribs, spars, and skin of graphite-epoxy for low weight and high stiffness.

The instrumentation was mostly on the upper surface (shown in Fig 3) with a few transducers on the lower surface to establish symmetry and zero angle of attack. There are 5 chordwise locations for the transducers, with chord C consisting of a few transducers near the edges of the control surfaces. Static and dynamic measurements were made separately, with a static orifice adjacent to each dynamic transducer. The locations of the static orifices are given in Table 1, and locations of the orifices for the dynamic transducers are given in Table 2. The static pressure tubing was also connected to the reference side of the corresponding dynamic orifices through 35 feet (10.7 m) of .020 inch (.51 mm) diameter tubing to damp out unsteady effects on the reference pressure.

Although ordinates were measured for this wing, it was concluded that the basic definition of a t/c=0.06 circular arc was adequate to describe the airfoil geometry of the wing and the measured ordinates were not published. It was noted (Ref 1) that the control surface had two degrees of twist, which was averaged by setting the inboard portion low and the outboard portion high.

As can been seen in Fig 1, the model was tested with the sidewall slots of the test section open. Some recent unpublished results for a model of about twice the root chord of this model and mounted directly to the wind tunnel wall have shown an order of ten percent influence of closing the slots on static lift curve slope (similar to those measured in Ref 23). Significantly less influence would be anticipated for this smaller model which was mounted on a splitter plate.

TEST CASES

The static Test Cases chosen for the Clipped Delta Wing (CDW) are given in Table 3, and the dynamic Test Cases are presented in Tables 4 and 5. The code, or point index, for the cases are designated with a two-digit value of the test Mach number, followed by an S for static or D for dynamic, and followed by a sequence number for each Mach number (Ref 1). The pitch cases are chosen to indicate trends with Mach number at zero angle of attack, trends with Mach number for small values of angle

of attack, and trends with angle of attack at one low and one transonic Mach number (including some cases with leading-edge vortex flows). The trailing edge control cases also illustrate trends with Mach number and static deflection amplitude of the trailing-edge control surface. The dynamic cases are chosen to evaluate unsteady effects at these static conditions. One feature of this data set is a relatively high Reynolds number for the test, of the order of 10×10^6 based on the average chord.

A sample data point for the static Test Cases is tabulated and shown in the composite plot of Fig 5. The data for the dynamic cases are also tabulated and shown in the plots of Figs 6 and 7 in terms of in-phase and out-of-phase parts (real and imaginary) of the pressure normalized by the amplitude of the dynamic motion, either pitch or control-surface oscillation (in radians). The phase reference is the input dynamic motion. More figures than are significant are retained in the Tables to accurately reproduce the phase angles of the original tabulations. For each of these cases, the data points are connected by straight lines for visual continuity only and the lines are not intended to be considered a fairing of the data. No further screening of bad points have been performed in this report. In the original data set, the output of bad transducers was set to zero.

The files included on the CD-ROM are ascii files and a readme file is included. The file for the static data is named cdwstat and a Fortran subprogram to read it, cdwstrd.f, is furnished. The dynamic data is on file cdwdynmc and the subprogram to read it is cdwdyrd.f. The data files consist of contiguous data points in the format shown in the figures.

Note that all of the tests for the CDW were conducted with the heavy gas, R-12, as the test medium. The ratio of specific heats, γ, is calculated to be 1.132 to 1.135 for the conditions of the test assuming 0.99 for the fraction of heavy gas in the heavy gas-air mixture. A value of 1.132 is suggested for use in computational comparisons. The corresponding value of Prandtl number is calculated to range from 0.77 to 0.78 for the conditions of this test.

FORMULARY

1 General Description of Model

1.1	Designation	Clipped Delta Wing (CDW)
1.2	Type	Semispan wing
1.3	Derivation	Simplified version of early SST with thicker airfoil (see Introduction)
1.4	Additional remarks	Shown mounted in tunnel in Fig 1
1.5	References	Ref 1 and 2 are the original source

2 Model Geometry

2.1	Planform	Trapezoidal
2.2	Aspect ratio	1.242 for panel
2.3	Leading edge sweep	50.4 deg.
2.4	Trailing edge sweep	Unswept
2.5	Taper ratio	0.1423
2.6	Twist	None
2.7	Wing centreline chord	63.55 inches (1614 mm)
2.8	Semi-span of model	45.08 inches (1145 mm)
2.9	Area of planform	1635.88 sq. in. (1.0554 sq. m)
2.10	Location of reference sections and definition of profiles	Six per cent circular arc airfoil section
2.11	Lofting procedure between reference sections	Constant per cent thickness airfoil
2.12	Form of wing-body junction	No fairing, sealed at splitter plate
2.13	Form of wing tip	Sharply cut off
2.14	Control surface details	Trailing edge control, 80% chord between 56.6% span and 82.9% span. Hinge line sealed, but side edges open. About two degrees twist in control surface, with inboard trailing edge low and outboard high
2.15	Additional remarks	See Fig 3 for overview
2.16	References	Ref 1 and 2

3 Wind Tunnel

3.1	Designation	NASA LaRC Transonic Dynamics Tunnel (TDT)
3.2	Type of tunnel	Continuous flow, single return
3.3	Test section dimensions	16 ft x 16 ft (4.064 x 4.064 m)
3.4	Type of roof and floor	Three slots each
3.5	Type of side walls	Two sidewall slots
3.6	Ventilation geometry	Constant width slots in test region
3.7	Thickness of side wall boundary layer	Some documentation in Ref 14. Model tested with splitter plate
3.8	Thickness of boundary layers at roof and floor	Not documented
3.9	Method of measuring velocity	Calculated from static pressures measured in plenum and total pressure measured upstream of entrance nozzle of test section
3.10	Flow angularity	Not documented, considered small
3.11	Uniformity of velocity over test section	Not documented, considered nearly uniform
3.12	Sources and levels of noise or turbulence in empty tunnel	Generally unknown. Some low speed measurements are presented in Ref 22. Cone transition measurements are presented in Ref 20 and 21.
3.13	Tunnel resonances	Unknown
3.14	Additional remarks	Tests performed in heavy gas, R-12. Ratio of specific heats, γ, is 1.132-1.135. For computations, 1.132 is recommended. For the conditions of this test, the Prandtl number is calculated to be 0.77-0.78
3.15	References on tunnel	Ref 14, 16, and 17

4 Model Motion

4.1	General description	Pitching about 65.22% of root chord for wing. Oscillation about control hinge line
4.2	Reference coordinate and definition of motion	Pitch about axis normal to freestream. Control oscillation about 80% chord line of wing
4.3	Range of amplitude	Pitch amplitude of 0.25 and 0.50 degrees. Control oscillation of 2, 4, and 6 degrees
4.4	Range of frequency	4, 8, and 16 Hz for wing pitch, and 8, 16, and 22 Hz for control surface oscillations
4.5	Method of applying motion	Pitch oscillations generated as spring-mass system driven by hydraulic actuator. Control surface oscillations driven by miniature hydraulic actuator at control surface
4.6	Timewise purity of motion	Not documented
4.7	Natural frequencies and normal modes of model and support system	First natural frequency was 28 Hz
4.8	Actual mode of applied motion including any elastic deformation	Not documented except for node lines for wind-off conditions. (Fig 4). Elastic deformations not expected to be significant
4.9	Additional remarks	None

5 Test Conditions

5.1	Model planform area/tunnel area	.05
5.2	Model span/tunnel height	.23
5.3	Blockage	Model less than 0.3%
5.4	Position of model in tunnel	Mounted from splitter plate on wall and in the center of the tunnel
5.5	Range of Mach number	0.40 to 1.12
5.6	Range of tunnel total pressure	530 to 1005 psf (25.4 to 48.1 kPa)
5.7	Range of tunnel total temperature	512 to 576 degrees Rankine (23 to 47° C)

5.8	Range of model steady or mean incidence	0 to 5.5 degrees
5.9	Definition of model incidence	From chord line of symmetric airfoil
5.10	Position of transition, if free	Transition strip used
5.11	Position and type of trip, if transition fixed	Grit strip 0.1 inch wide (2.5 mm) at 8 % chord on upper and lower surfaces. Number 70 grit from root to midspan and number 90 from midspan to tip (number is approximately grains per inch (per 25.4 mm))
5.12	Flow instabilities during tests	None defined
5.13	Changes to mean shape of model due to steady aerodynamic load	Not measured but considered very stiff
5.14	Additional remarks	Tests performed in heavy gas, R-12. Ratio of specific heats, γ, is 1.132-1.135. For computations, 1.132 is recommended. For the conditions of this test, the Prandtl number is calculated to be 0.77-0.78
5.15	References describing tests	Ref 1 and 2

6 Measurements and Observations

6.1	Steady pressures for the mean conditions	yes
6.2	Steady pressures for small changes from the mean conditions	yes
6.3	Quasi-steady pressures	no
6.4	Unsteady pressures	yes
6.5	Steady section forces for the mean conditions by integration of pressures	no
6.6	Steady section forces for small changes from the mean conditions by integration	no
6.7	Quasi-steady section forces by integration	no
6.8	Unsteady section forces by integration	no
6.9	Measurement of actual motion at points of model	no
6.10	Observation or measurement of boundary layer properties	no
6.11	Visualisation of surface flow	no
6.12	Visualisation of shock wave movements	no
6.13	Additional remarks	no

7 Instrumentation

7.1	Steady pressure	
7.1.1	Position of orifices spanwise and chordwise	7 to 16 chordwise locations at 5 spanwise stations. See Fig 3 and Table 1
7.1.2	Type of measuring system	Scani-valve
7.2	Unsteady pressure	
7.2.1	Position of orifices spanwise and chordwise	7 to 16 chordwise locations at 5 spanwise stations. See Fig 3 and Table 2. Slightly different locations than steady.
7.2.2	Diameter of orifices	.056 inches (1.4 mm)
7.2.3	Type of measuring system	In situ pressure gages
7.2.4	Type of transducers	Kulite
7.2.5	Principle and accuracy of calibration	Calibrated dynamically using method of Ref 24. Also statically calibrated through reference tubes

7.3	Model motion	
	7.3.1 Method of measuring motion reference coordinate	Undocumented
	7.3.2 Method of determining spatial mode of motion	Wind-off verification with accelerometers
	7.3.3 Accuracy of measured motion	Undocumented
7.4	Processing of unsteady measurements	
	7.4.1 Method of acquiring and processing measurements	Analog signals digitized at about 940 samples/sec for 10-30 seconds depending on frequency
	7.4.2 Type of analysis	Fourier analysis
	7.4.3 Unsteady pressure quantities obtained and accuracies achieved	Amplitude and phase of each pressure signal. Accuracy not specified
	7.4.4 Method of integration to obtain forces	None
7.5	Additional remarks	None
7.6	References on techniques	Data system overview for test given in Ref 15

8 Data Presentation

8.1	Test Cases for which data could be made available	See Ref 1 and 2
8.2	Test Cases for which data are included in this document	See Tables 3 and 4
8.3	Steady pressures	Available for each Test Case
8.4	Quasi-steady or steady perturbation pressures	Steady pressures measured for several angles of attack
8.5	Unsteady pressures	Primary data. First harmonic only. No time histories saved. C_p magnitude and phase of Ref 1 converted to real and imaginary parts and normalized by amplitude of oscillation (in radians)
8.6	Steady forces or moments	Some static hinge moments for control surface plotted in Ref 1. No other force measurements
8.7	Quasi-steady or unsteady perturbation forces	None
8.8	Unsteady forces and moments	None
8.9	Other forms in which data could be made available	None
8.10	References giving other representations of data	Ref 1-2 and 8-11

9 Comments on Data

9.1	Accuracy	
	9.1.1 Mach number	Not documented
	9.1.2 Steady incidence	Zero set by pressure difference. Accuracy of other values unknown
	9.1.3 Reduced frequency	Should be accurate
	9.1.4 Steady pressure coefficients	Not documented
	9.1.5 Steady pressure derivatives	None
	9.1.6 Unsteady pressure coefficients	Not documented, but each gage individually calibrated dynamically and monitored statically
9.2	Sensitivity to small changes of parameter	None indicated. Amplitudes of oscillation varied in test
9.3	Non-linearities	Plotted (Ref 2) hinge moments show some nonlinearity. Many flow conditions involve shock waves; some with leading edge vortex flows
9.4	Influence of tunnel total pressure	Not evaluated. Most of the test at constant dynamic pressure

9.5	Effects on data of uncertainty, or variation, in mode of model motion	Unknown, not expected to be appreciable. Wind-off measurements shown in Fig 4
9.6	Wall interference corrections	None applied
9.7	Other relevant tests on same model	None
9.8	Relevant tests on other models of nominally the same shapes	Flutter tests on similar planform but with thinner airfoil presented in Ref 4-7
9.9	Any remarks relevant to comparison between experiment and theory	Leading edge vortex forms near 3 degrees angle of attack. Some cases have both vortex flow and shock waves. Test Reynolds number included for each Test Case. Reduced frequency based on root semichord, 31.775 inches (807.1 mm) for all Test Cases
9.10	Additional remarks	Wing mostly instrumented on one side. Upper and lower surface data assembled from varying angle of attack
9.11	References on discussion of data	Ref 1-2 and 8-11

10 Personal Contact for Further Information

Head, Aeroelasticity Branch
Mail Stop 340
NASA Langley Research Center
Hampton, VA 23681-2199 USA

Phone: +1-(757)-864-2820
FAX: +1-(757)-864-8678

LIST OF REFERENCES

1 Hess, Robert W.; Cazier, F. W., Jr.; and Wynne, Eleanor C.: *Steady and Unsteady Transonic Pressure Measurements on a Clipped Delta Wing for Pitching and Control-Surface Oscillations.* NASA TP-2594, Oct. 1986.

2 Hess, R. W.; Cazier, F. W.,Jr.; and Wynne, E. C.: *Static and Unsteady Pressure Measurements on a 50 degree Clipped Delta Wing at M = 0.9.* AIAA Paper 82-0686, 1982. Also available as NASA TM-83297, 1982.

3 Bhatia, Kumar G.; and Wertheimer, Jiri: *Aeroelastic Challenges for a High Speed Civil Transport.* AIAA Paper 93-1478, May 1993.

4 Sandford, Maynard C.; Abel, Irving; and Gray, David L.: *Development and Demonstration of a Flutter-Suppression System Using Active Controls.* NASA TR R-450, 1974.

5 Sandford, Maynard C.; Ruhlin, Charles L.; and Abel, Irving: *Transonic Flutter Study of a 50.5-Deg. Cropped-Delta Wing with Two Rearward-Mounted Nacelles.* NASA TN D-7544, 1974.

6 Goetz, Robert C.: *Exploratory Study of Buffet and Stall Flutter of Space Vehicle Wing Concepts.* NASA LWP-872, May 1970.

7 Ruhlin, Charles L.; Destuynder, Roger M.; and Gregory, Richard A.: *Some Wind Tunnel Wall Effects on Transonic Flutter.* Journal of Aircraft, vol. 12, no. 3, Mar. 1975, pp 162-167.

8 Yates, E. Carson, Jr.; Cunningham, Herbert J.; Desmarais, Robert N.; Silva, Walter A.; and Drobenko, Bohdan: *Subsonic Aerodynamic and Flutter Characteristics of Several Wings Calculated by the SOUSSA P1.1 Panel Method.* AIAA Paper 82-0727, May 1982.

9 Guruswamy, Guru P.; and Obayashi, Shigeru: *Transonic Aeroelastic Computations on Wings Using Navier-Stokes Equations.* Paper No. 22 in "Transonic Unsteady Aerodynamics and Aeroelasticity", AGARD-CP-507, Mar. 1992.

10 Obayashi, Shigeru; and Guruswamy, Guru P.: *Unsteady Shock-Vortex Interaction on a Flexible Delta Wing.* Journal of Aircraft, vol. 29, no. 5, Sept.-Oct. 1992, pp 790-798.

11 Obayashi, Shigeru; and Guruswamy, Guru P.: *Navier-Stokes Computations for Oscillating Control Surfaces.* Journal of Aircraft, vol. 31, no. 3, May-June 1994, pp. 631-636.

12 Bennett, Robert M.; Batina, John T.; and Cunningham, H. J.: *Wing-Flutter Calculations with the CAP-TSD Unsteady Transonic Small-Disturbance Program.* Journal of Aircraft, vol. 26, no. 9, Sep. 1989, pp. 876-882.

13 Bennett, Robert M.; Walker, Charlotte, E.: *Computational Test Cases For a Clipped Delta Wing with Pitching and Trailing-Edge Control Surface Oscillations.* NASA/TM-1999-209104, Mar.1999.

14 Aeroelasticity Branch Staff: *The Langley Transonic Dynamics Tunnel.* LWP-799, Sep. 1969.

15 Cole, Patricia H.: *Wind Tunnel Real-Time Data Acquisition System.* NASA TM 80081, 1979.

16 Cole, Stanley, R.; and Rivera, Jose, A, Jr.: *The New Heavy Gas Testing Capability in the NASA Langley Transonic Dynamics Tunnel.* Paper No. 4, presented at the Royal Aeronautical Society Wind Tunnels and Wind Tunnel Test Techniques Forum, Churchill College, Cambridge, UK, Apr. 1997.

17 Corliss, James M.; and Cole, Stanley R.: *Heavy Gas Conversion of the NASA Langley Transonic Dynamics Tunnel.* AIAA Paper 98-2710, June 1998.

18 Wieseman, Carol D.; and Hoadley, Sherwood, T.: *Versatile Software Package for Near Real-Time Analysis of Experimental Data.* AIAA Paper 98-2722, June 1998.

19 Bryant, C.; and Hoadley , S. T.: *Open Architecture Dynamic Data System at Langley's Transonic Dynamics Tunnel.* AAIA Paper 98-0343, Jan. 1998.

20 Dougherty, N. Sam, Jr.: *Influence of Wind Tunnel Noise on the Location of Boundary-Layer Transition on a Slender Cone at Mach Numbers from 0.2 to 5.5. Volume I. - Experimental Methods and Summary of Results. Volume II. - Tabulated and Plotted Data.* AEDC--TR-78-44, March 1980.

21 Dougherty, N. Sam, Jr.; and Fisher, D. F.: *Boundary-Layer Transition on a 10-Deg. Cone: Wind Tunnel/Flight Correlation.* AIAA Paper 80-0154, January 1980.

22 Sleeper, Robert K.; Keller, Donald F.; Perry, Boyd, III; and Sandford, Maynard C.: *Characteristics of Vertical and Lateral Tunnel Turbulence Measured in Air in the Langley Transonic Dynamics Tunnel.* NASA TM 107734, March 1993.

23 Lambourne, N.; Destuynder, R.; Kienappel, K.; and Roos, R.: *Comparative Measurements in Four European Wind Tunnels of the Unsteady Pressures on an Oscillating Model (The NORA Experiments).* AGARD Report No. 673, Feb. 1980.

24 Bolt, Pamela C.; Hess, Robert W.; and Davis William T.: *Portable Dynamic Pressure Generator for Static and Dynamic Calibration of In-Situ Pressure Transducers.* NASA TM 85687, 1983.

ACKNOWLEDGMENT

The considerable assistance of Charlotte E. Walker in generating the tables and figures for this report is gratefully acknowledged.

Table 1. Orifice Locations for Steady Measurements

Chord A	Chord B	Chord C	Chord D	Chord E
y/s				
0.332	0.541	0.587	0.694	0.851
x/c				
0.0778	0.0687	0.0818	0.0675	0.2070
0.1264	0.1282	0.1318	0.1151	0.2559
0.2020	0.2529	0.2099	0.1980	0.3016
0.2523	0.3041	0.7875	0.2559	0.3537
0.3023	0.3531	0.8522	0.3041	0.4583
0.3519	0.4530	0.9017	0.3545	0.5562
0.4510	0.5036	0.9514	0.4537	0.6074
0.5523	0.5534		0.5025	0.6577
0.6025	0.6040		0.5527	0.7071
0.6515	0.6528		0.6038	0.7975
0.6991	0.7030		0.6538	
0.7813	0.7694		0.7025	
0.8505	0.8967		0.7754	
0.9001	0.9512		0.8553	
0.9596			0.9037	
			0.9526	

Table 2. Orifice Locations for Unsteady Measurements

Chord A	Chord B	Chord C	Chord D	Chord E
y/s				
0.337	0.546	0.590	0.698	0.856
x/c				
0.0731	0.0681	0.0767	0.0754	0.1955
0.1120	0.1237	0.1271	0.1237	0.2458
0.1974	0.2485	0.1993	0.1980	0.2915
0.2478	0.3004	0.7802	0.2502	0.3454
0.2987	0.3481	0.8514	0.3001	0.4519
0.3486	0.4487	0.9016	0.3476	0.5497
0.4477	0.4997	0.9511	0.4495	0.6025
0.5506	0.5500		0.4974	0.6545
0.6009	0.6014		0.5484	0.7049
0.6459	0.6494		0.6007	0.7808
0.6979	0.6995		0.6514	
0.7805	0.7747		0.7000	
0.8500	0.8964		0.7795	
0.8996			0.8547	
0.9495			0.9033	
			0.9522	

Table 3. Static Test Cases

Test Case No.	Point (Code[1])	M	α_o deg.	δ_o deg.	Comments
9E1	.40-S-1	.399	.05	0.	
9E2	.88-S-1	.883	.05	0.	
9E3	.90-S-1	.899	.05	0.	Versus
9E4	.92-S-1	.921	.05	0.	M @ α_o=0°
9E5	.94-S-1	.944	.05	0.	
9E6	. 96-S-1	.965	.00	0.	
9E7	1.12-S-1	1.120	.00	0.	
9E8	.40-S-6	.400	1.03	0.	
9E9	.90-S-5	.909	.99	0.	Versus
9E10	.94-S-6	.943	.97	0.	M @ α_o = 1°
9E11	1.12-S-6	1.120	.99	0.	
9E12	.40-S-11	.404	3.04	0.	
9E13	.40-S-15	.403	5.04	0.	Versus
9E14	.90-S-19	.900	2.99	0.	α_o @M
9E15	.90-S-38	.901	4.24	0.	
9E16	.40-S-3	.406	.05	4.	
9E17	.90-S-2	.898	.05	2.	Versus
9E18	.90-S-3	.896	.05	4.	δ_o @ α_o = 0
9E19	.94-S-3	.944	.05	4.	
9E20	1.12-S-3	1.120	.00	4.	
9E21	.90-S-21	.901	2.99	4.	Versus
9E22	.90-S-24	.896	2.99	-4.	δ_o @ α_o

[1] Ref 1

Table 4. Test Cases for Pitching Oscillations, $\delta_o = 0$

Test Case No.	Point (Code[1])	M	α_o deg.	θ deg.	f Hz	k	Comments
9E23	.40-D-5	.403	.05	.47	4.00	.194	
9E24	.88-D-5	.885	.05	.48	7.98	.173	
9E25	.90-D-5	.904	.00	.46	7.99	.167	Versus M
9E26	.92-D-5	.921	.05	.47	7.97	.166	
9E27	.94-D-5	.945	.05	.47	7.98	.162	
9E28	.96-D-4	.961	.04	.50	7.99	.158	
9E29	1.12-D-5	1.120	.00	.47	8.00	.136	
9E30	.90-D-2	.905	.00	.24	7.99	.168	Lower θ
9E31	.90-D-4	.904	.00	.50	4.01	.084	Lower k
9E32	.90-D-6	.909	.00	.46	16.01	.335	Higher k
9E33	.40-D-24	.403	5.02	.50	4.00	.189	Higher α_o
9E34	.90-D-29	.902	3.97	.46	7.99	.169	

[1] Ref 1

Table 5. Test Cases for Control Surface Oscillations, $\delta_o = 0$

Test Case No.	Point (Code[1])	M	α_o deg.	δ deg.	f Hz	k	Comments
9E35	.40-D-32	.405	.05	3.90	7.99	.376	
9E36	.88-D-34	.878	.05	3.88	16.00	.350	
9E37	.90-D-35	.901	.05	4.00	16.00	.338	Versus M
9E38	.92-D-33	.923	.05	3.93	15.98	.337	
9E39	.94-D-34	.942	.05	3.96	15.98	.326	
9E40	.96-D-10	.960	.05	4.54	16.00	.315	
9E41	1.12-D-11	1.120	.00	4.37	16.01	.273	
9E42	.90-D-32	.898	.05	3.48	7.99	.170	Lower k
9E43	.92-D-36	.924	.05	3.89	22.00	.459	Higher k
9E44	.90-D-34	.898	.05	1.97	16.00	.339	Lower δ
9E45	.90-D-36	.899	.04	5.82	16.01	.340	Higher δ
9E46	.90-D-59	.901	2.99	4.39	16.01	.337	Higher α_o

[1] Ref 1

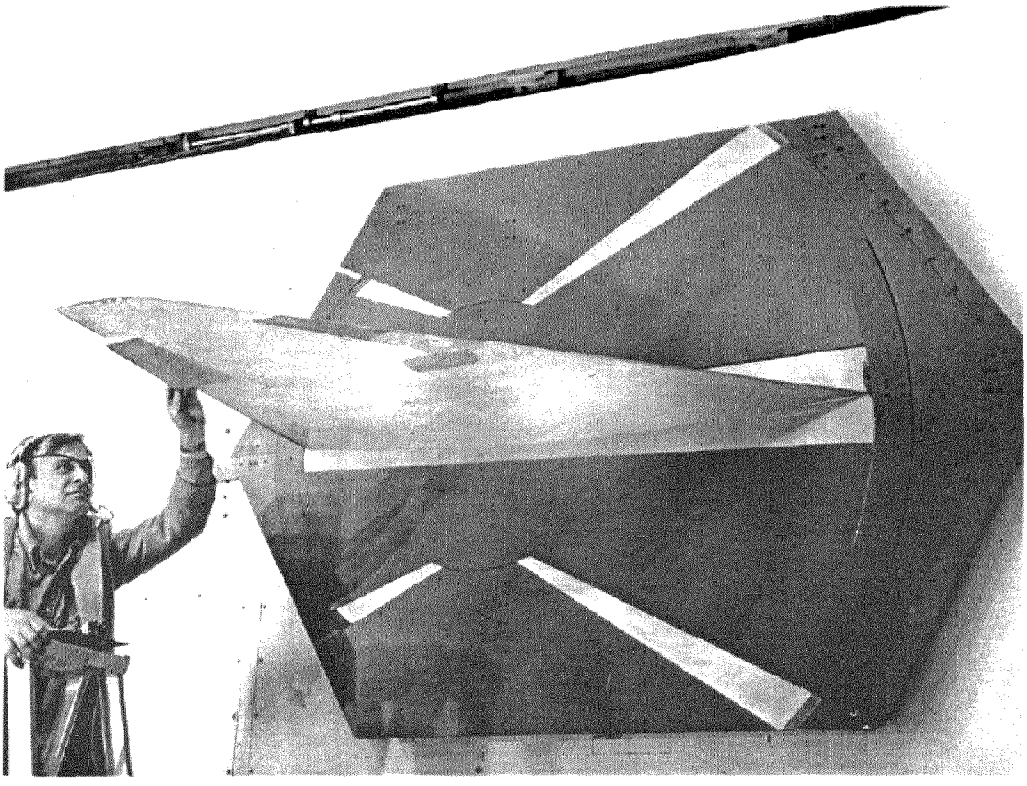

Figure 1. Clipped delta wing installed in wind tunnel.

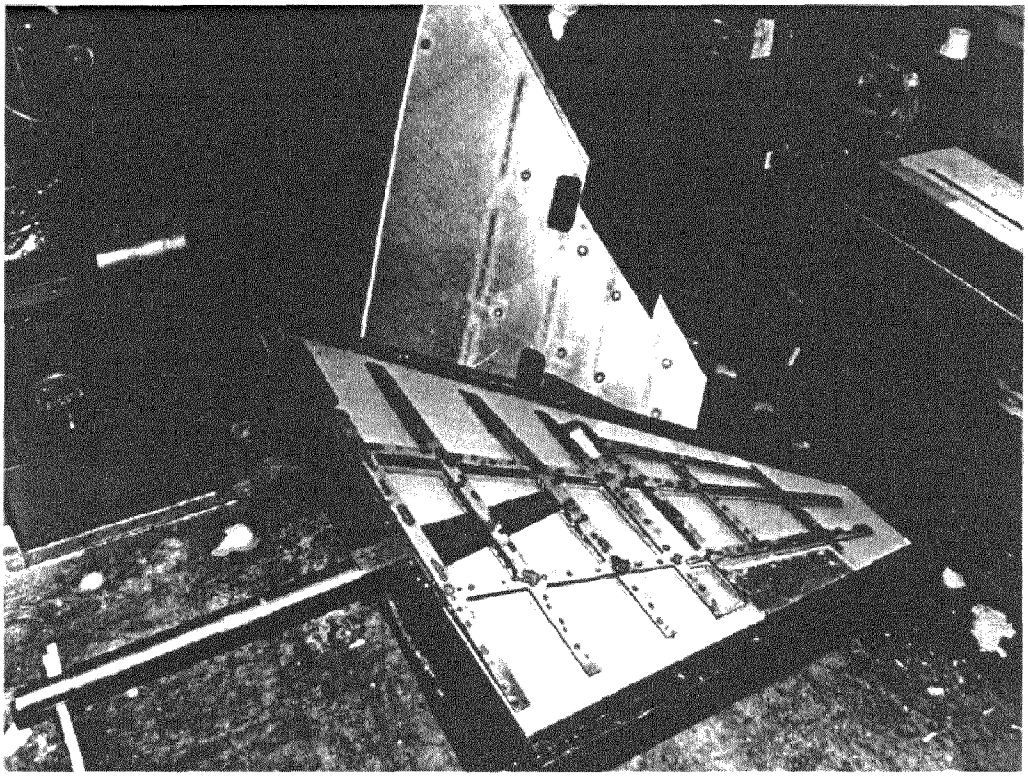

Figure 2. Construction of clipped delta wing.

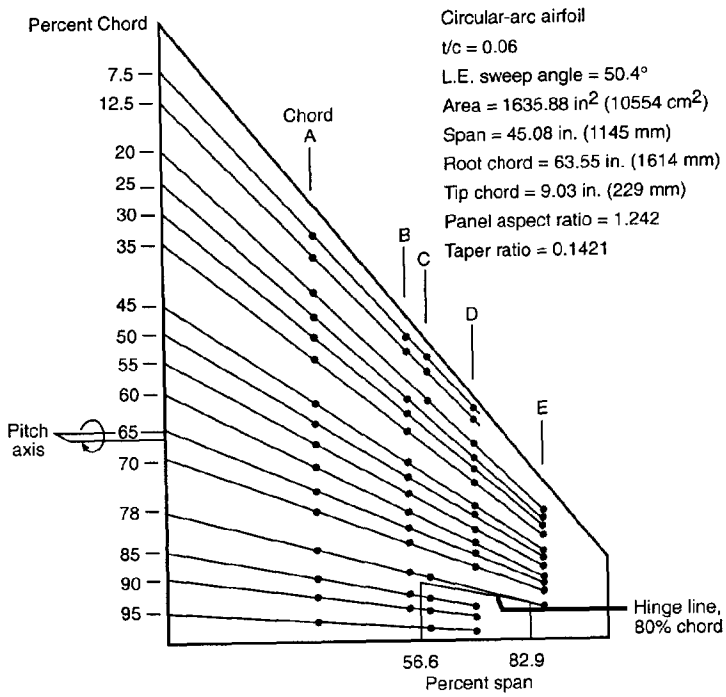

Figure 3. Planform geometry and instrumentation layout.

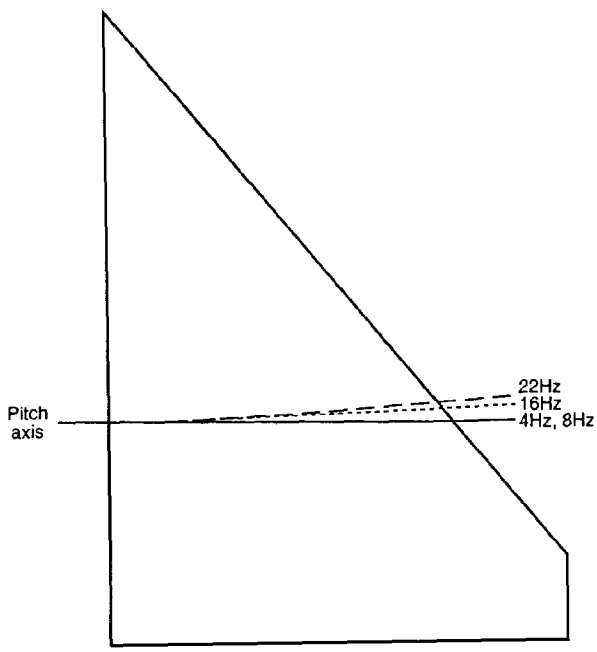

Figure 4. Node lines for test frequencies in still air.

.90-S-1

MACH	q psf	To deg R	H psf	ALPHAo deg	THETA deg	DELTA deg	RN
0.899	191.2	565.3	651.8	0.05	0.00	0.00	9.77 *10**6

y/s = 0.332			y/s = 0.541			y/s = 0.587			y/s = 0.694			y/s = 0.851		
x/c	Cpu	Cpl	x/c	Cpu	Cpl	x/c	Cpu	Cpl	x/c	Cpu	Cpl	x/c	Cpu	Cpl
.0778	0.0217		.0687	0.0049		.0818	0.0229		.0675	-.0528		.2070	-.2689	
.1264	-.0318		.1282	-.0788		.1318	-.0596		.1151	-.0572		.2559	-.3260	
.2020	-.0802		.2529	-.1548		.2099	-.1477		.1980	-.1748		.3016	-.2912	
.2523	-.1134		.3041	-.2251		.7875	-.1491		.2559	-.2408		.3537	-.3057	
.3023	-.1580		.3531	-.2484		.8522	-.0710		.3041	-.2481		.4583	-.4098	
.3519	-.1620		.4530	-.2859		.9017	0.0186		.3545	-.2905		.5562	-.4368	
.4510	-.2456		.5036	-.3258		.9514	0.0988		.4537	-.3831		.6074	-.3943	
.5523	-.2424		.5534	-.3261					.5025	-.3628		.6577	-.3388	
.6025	-.3011		.6040	-.3542					.5527	-.3760		.7071	-.2408	
.6515	-.3778		.6528	-.3646					.6038	-.3990		.7975	-.0879	
.6991	-.3374		.7030	-.3350					.6538	-.3987				
.7813	-.2514		.7694	-.1980					.7025	-.3588				
.8505	-.1069		.8967	0.0138					.7754	-.1191				
.9001	-.0362								.8553	-.0617				
.9596	0.0812								.9037	0.0126				
									.9526	0.0999				

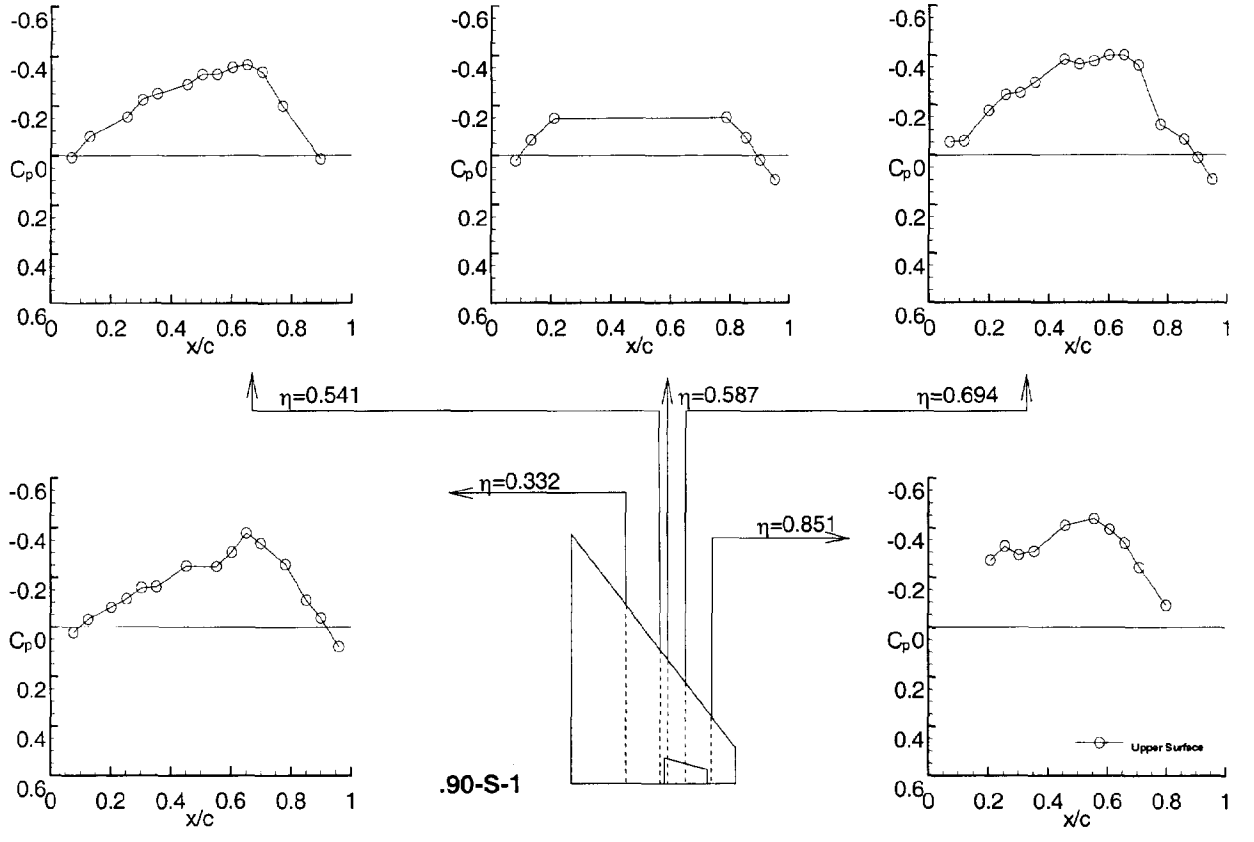

Figure 5. Static case, Test Case number 9E3 (point .90-S-1).

.90-D-5

MACH	q psf	To deg R	H psf	ALPHAo deg	THETA deg	DELTA deg	RN
0.904	200.3	566.2	679.5	0.00	0.46	0.00	10.13*10**6

f = 7.99 Hz k = 0.167

y/s = 0.337

	Upper		Lower	
x/c	Real	Imag	Real	Imag
.0731	-2.4667	0.7920		
.1120	-2.1392	0.5334		
.1974	-2.1072	0.3867		
.2478	-2.1140	0.2596		
.2987	-1.0684	0.0766		
.3486	-2.2901	0.0880		
.4477	-1.8757	-0.1377		
.5506	-2.0993	-0.1542		
.6009	-2.1938	-0.4623		
.6459	-2.5171	-0.6136		
.6979	-4.0662	-0.8791		
.7805	0.2918	-3.4253		
.8500	0.8783	-0.8655		
.8996	0.7067	-0.4199		
.9495	0.4162	-0.1668		

y/s = 0.546

	Upper		Lower	
x/c	Real	Imag	Real	Imag
.0681	-3.8789	1.2007		
.1217	-3.2047	0.8407		
.2485	-2.4548	0.4240		
.3004	-2.0958	0.3020		
.3481	-1.3275	0.2174		
.4487	-2.9393	0.0359		
.4997	-2.1027	-0.0992		
.5500	-2.4586	0.1935		
.6014	-2.6647	0.0651		
.6494	-4.7044	-0.1889		
.6995	-4.5903	-2.0919		
.7747	1.0737	-2.1090		
.8964	0.3784	-0.5410		

y/s = 0.590

	Upper		Lower	
x/c	Real	Imag	Real	Imag
.0767	-3.6778	1.2163		
.1271	-3.2311	0.9326		
.1993	-2.9437	0.7558		
.7802	1.6063	-1.4734		
.8514	0.3705	-0.2741		
.9016	0.6694	-0.3851		
.9511	0.6307	-0.0754		

y/s = 0.698

	Upper		Lower	
x/c	Real	Imag	Real	Imag
.0754	-2.2762	0.2674		
.1237	-4.1315	1.0378		
.1980	-3.8566	0.7217		
.2502	0.6121	-3.4714		
.3001	-1.4630	0.1409		
.3476	-3.2697	0.3494		
.4495	-3.1492	0.3032		
.4974	-2.9312	0.3495		
.5484	-2.5658	0.0134		
.6007	-3.1078	-0.1955		
.6514	-4.3593	-1.4164		
.7000	-2.1524	-2.9626		
.7795	0.6742	-0.4254		
.8547	0.5982	-0.1213		
.9033	0.5532	-0.1917		
.9522	0.6080	-0.0529		

y/s = 0.856

	Upper		Lower	
x/c	Real	Imag	Real	Imag
.1955	-3.1322	0.5975		
.2458	-4.2549	0.8271		
.2915	-4.8539	1.0672		
.3454	-1.7394	3.0372		
.4519	-3.6992	0.0323		
.5497	-4.8832	-0.6950		
.6025	-4.2134	-2.8634		
.6545	1.1374	-4.1181		
.7049	3.4864	-0.9446		
.7808	1.0075	0.0537		

(a) Tabulated data for 9E25

Figure 6. Pitching oscillation, Test Case number 9E25 (point 90-D-5).

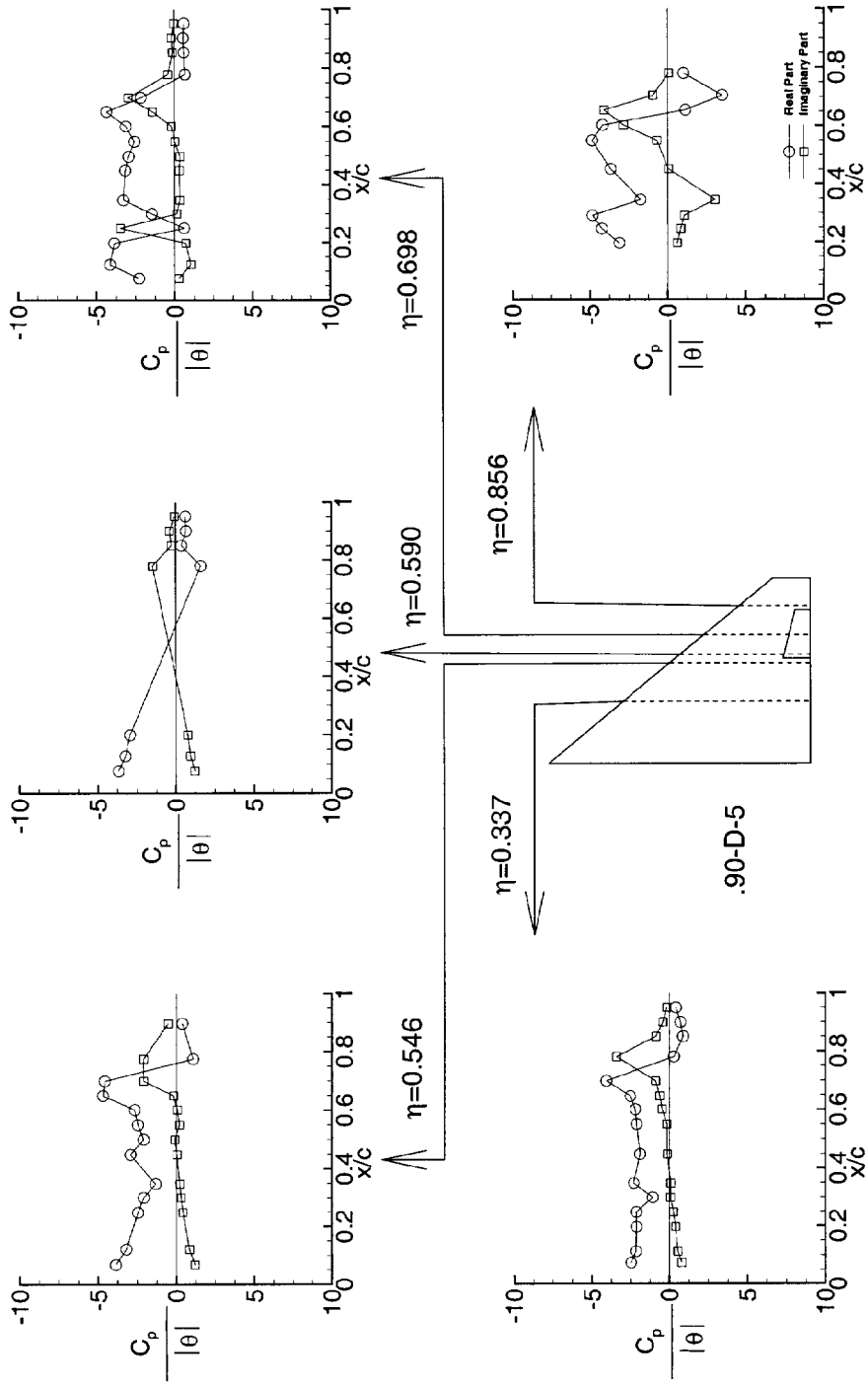

(b) Plot of data for 9E25

Figure 6. Concluded.

.90-D-35

MACH	q psf	To deg R	H psf	ALPHAo deg	THETA deg	DELTA deg	RN
0.901	192.0	565.2	654.1	0.05	0.00	4.00	9.84*10**6

f = 16.00 Hz k = 0.338

y/s = 0.337

	Upper		Lower	
x/c	Real	Imag	Real	Imag
.0731	-0.3013	0.0483		
.1120	-0.2954	0.0389		
.1974	-0.2567	0.0238		
.2478	-0.2545	0.0151		
.2987	-0.0003	0.0014		
.3486	-0.2807	0.0059		
.4477	-0.2034	0.0025		
.5506	-0.1782	-0.0175		
.6009	-0.2402	0.0139		
.6459	-0.3362	0.0563		
.6979	-0.2748	-0.0416		
.7805	0.0218	-0.1008		
.8500	0.0343	-0.0304		
.8996	0.0133	-0.0053		
.9495	-0.0012	0.0085		

y/s = 0.546

	Upper		Lower	
x/c	Real	Imag	Real	Imag
.0681	-0.1346	0.0014		
.1217	-0.3132	0.0346		
.2485	-0.2704	0.0128		
.3004	-0.2546	0.0142		
.3481	-0.0008	0.0012		
.4487	-0.4544	0.0703		
.4997	-0.2319	0.0081		
.5500	-0.2116	-0.0122		
.6014	-0.2879	-0.0030		
.6494	-0.3553	-0.1293		
.6995	-0.2401	-0.1589		
.7747	0.0796	-0.0610		
.8964	0.0180	-0.0142		

y/s = 0.590

	Upper		Lower	
x/c	Real	Imag	Real	Imag
.0767	-0.7556	0.1278		
.1271	-0.5800	0.0825		
.1993	-0.4027	0.0466		
.7802	0.0688	-0.0562		
.8514	-0.0005	0.0028		
.9016	0.0258	-0.0002		
.9511	0.0037	0.0123		

y/s = 0.698

	Upper		Lower	
x/c	Real	Imag	Real	Imag
.0754	-0.2543	0.0182		
.1237	-0.1991	0.0010		
.1980	-0.2930	0.0195		
.2502	-0.3981	0.0489		
.3001	-0.0006	0.0013		
.3476	-0.4392	0.0547		
.4495	-0.3093	0.0070		
.4974	-0.3492	0.0140		
.5484	-0.3953	0.0048		
.6007	-0.4157	-0.0673		
.6514	-0.3653	-0.2793		
.7000	0.2386	-0.3260		
.7795	0.0521	-0.0096		
.8547	0.0902	0.0036		
.9033	0.0968	-0.0106		
.9522	-0.0052	0.0068		

y/s = 0.856

	Upper		Lower	
x/c	Real	Imag	Real	Imag
.1955	-0.2882	0.0252		
.2458	-0.4349	0.0220		
.2915	-0.3566	0.0056		
.3454	-0.4440	0.0008		
.4519	-0.4439	0.0108		
.5497	-0.3540	-0.2255		
.6025	0.2054	-0.2757		
.6545	0.4322	-0.1017		
.7049	0.1496	0.0151		
.7808	0.0026	0.0199		

(c) Tabulated data for 9E37

Figure 7. Control surface oscillation, Test Case number 9E37 (point 90-D-35).

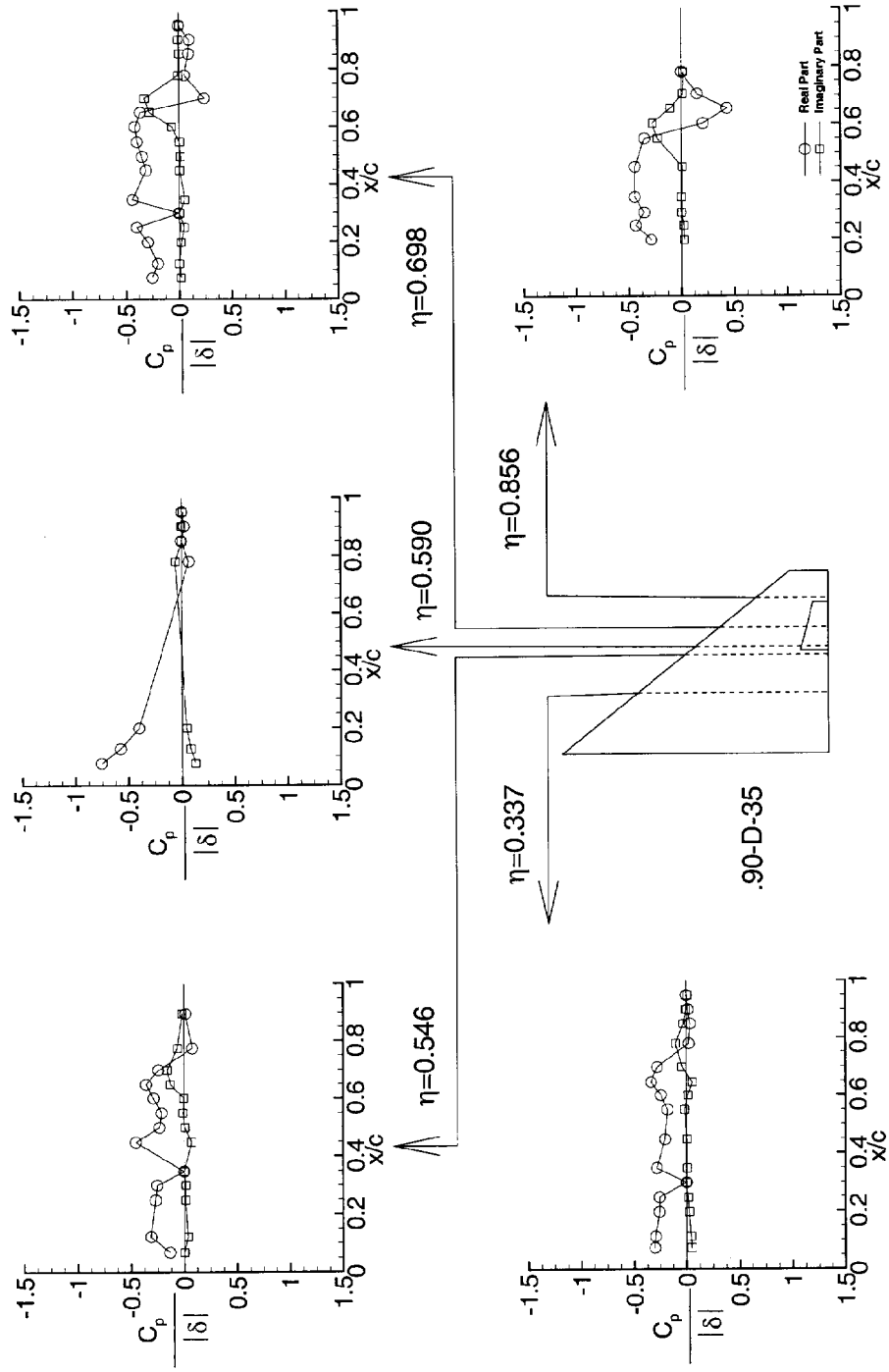

(d) Plot of data for 9E37

Figure 7. Concluded.